CORRELATIVE PROBE ELECTRON MICROSCOPY ANALYSIS OF PLASMA-TREATED GALLIUM-DOPED ZINC OXIDE NANORODS

[1]David RUTHERFORD, [2]Zdenek REMES, [3]Julia MICOVA, [1]Egor UKRAINTSEV, [1]Bohuslav REZEK

[1]*Faculty of Electrical Engineering, Czech Technical University in Prague, Prague, Czech Republic, EU*
[2]*Institute of Physics, Czech Academy of Sciences, Prague, Czech Republic, EU*
[3]*Institute of Chemistry, Slovak Academy of Sciences, Bratislava, Slovakia, EU*

Abstract

Correlative Probe Electron Microscopy (CPEM) was used to investigate the topographical and electronic emission properties of gallium-doped zinc oxide nanorods (ZnO:Ga) after low pressure hydrogen or oxygen plasma treatment. Simultaneous secondary electron (SE) and back-scattered electron (BSE) emission information from the same nanorods enabled true correlation with the topographical information obtained by atomic force microscopy (AFM). All nanorods were analyzed *in-situ* on the same substrate using the same experimental parameters which allowed for accurate comparison. ZnO:Ga nanorods displayed the largest SE emission intensity as well as the greatest BSE emission intensity. Hydrogen plasma treatment reduced both SE and BSE emission intensity, whereas oxygen plasma treatment only reduced SE emission. These effects may help elucidate various optical as well as biological interactions of ZnO:Ga nanorods.

keywords: Correlative microscopy, SEM, AFM, ZnO nanorods, plasma treatment

1. INTRODUCTION

Correlative microscopy combines the information measured from two or more typically separate techniques from the same region of interest, analyzed under the same conditions [1, 2]. The underlying principle is to simultaneously detect, acquire and combine the signals from the separate analyses to reveal new information that would otherwise not have been possible. Correlative Probe and Electron Microscopy (CPEM) is a new technology which integrates the techniques of Atomic Force Microscopy (AFM) and Scanning Electron Microscopy (SEM) [3]. High resolution topographical 3D images can be obtained using AFM alongside information on the electrical, mechanical and magnetic properties of a sample but the rate at which information is acquired is slow. In contrast, scan speeds are typically much faster using SEM and can gather electronic, morphological and chemical properties but the information is limited to a 2D image. The combination of these two techniques offers the possibility to improve the understanding of the analyzed material through the creation of a 3D CPEM image that combines both topographical and electronic information. In particular, complex materials subjected to surface treatments would be ideal candidates to benefit from such a correlative approach.

Zinc oxide (ZnO) is a wide band gap semi-conductor whose properties can be enhanced with the incorporation of a dopant during the synthesis process, and elements that have similar ionic radii, such as gallium, are the most promising candidates [4]. Treatment of doped materials by plasma is a quick and effective method to tailor the surface for particular applications [5]. Hydrogen plasma has been shown to passivate defects in ZnO [6, 7], whereas oxygen plasma is typically used for the removal of contamination from surfaces [8] and reducing contact angle/increasing wettability [9], including zinc oxide doped with gallium (ZnO:Ga, [10]). We previously showed that plasma treatment enhanced the antibacterial and photocatalytic effects of ZnO:Ga largely due to increased surface roughness which was measured using AFM operating at ambient pressure and room

temperature [11]. SEM analysis of plasma-treated ZnO:Ga revealed the presence of surface features thought to be due to etching and removal of material caused by ion bombardment during plasma treatment. Whilst one can infer that the increased roughness measured by AFM outside vacuum from plasma-treated samples could be due to the presence of increased number of surface features observed by SEM under vacuum, true correlation of the information from both analyses was not possible because the analyses were performed separately on different ZnO:Ga nanorods.

In the current work, we perform true *in-situ* correlation of the topography and electronic emission of ZnO:Ga and the plasma-treated nanorods to provide new information about the surface structure. 3D CPEM images that overlay the secondary electron (SE) and back scattered electron (BSE) signal intensity detected using SEM onto the topographical information obtained using AFM from precisely the same nanorods reveal differences in the maximum intensity of electronic emission relative to surface topography.

2. METHODOLOGY

2.1 ZNO:GA SYNTHESIS

Gallium-doped zinc oxide (ZnO:Ga) was prepared using the hydrothermal growth technique [3] and a schematic diagram of the process can be seen in **Figure 1** (a). Briefly, stoichiometric amounts of zinc nitrate hexahydrate and gallium nitrate hydrate (Sigma Aldrich) were mixed together at room temperature. After 15 minutes of continuous stirring, hexamethylenetetramine (HMTA) solution was added whilst stirring of the mixture continued. Once the mixture was uniform and homogenous, the temperature was increased to 90°C for 3 h. The product was then removed from the solution by centrifugation and washed with deionized water (dH$_2$O) to remove any unreacted precursor. This process was repeated a further two times before lyophilization to remove any water from within the ZnO:Ga structure.
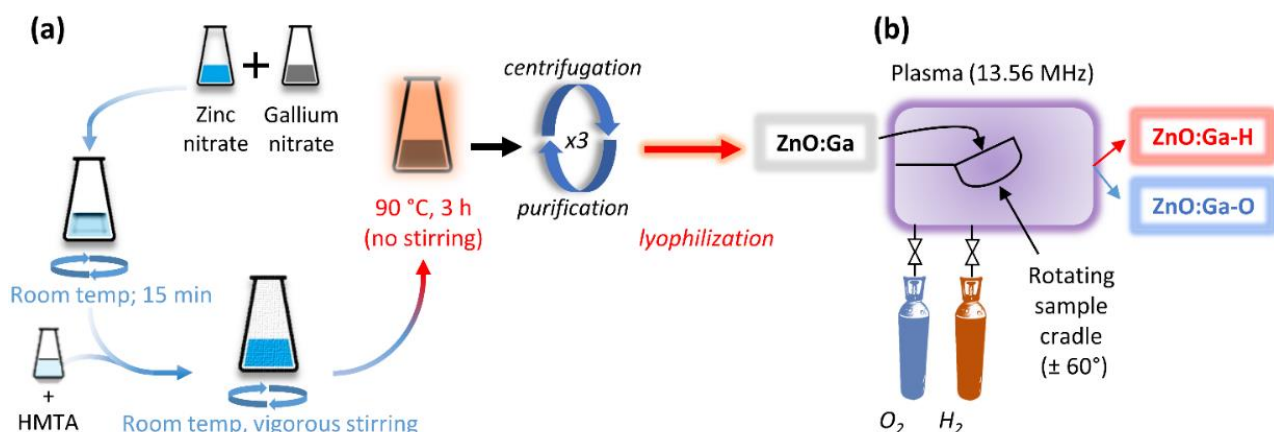
Figure 1 Schematic diagram of (a) ZnO:Ga synthesis by the hydrothermal growth technique and (b) subsequent plasma treatment of ZnO:Ga using either oxygen or hydrogen

2.2 PLASMA TREATMENT

Plasma treatment of ZnO:Ga synthesized by hydrothermal growth was performed at low pressure using an rf-ICP system (SVCS Process Innovation s.r.o) with custom quartz sample cradle (**Figure 1 (b)**) which rocked the material from side to side and ensured homogenous plasma treatment for a duration of 30 min [6]. Two separate gases were utilized for the plasma feed gas: pure H$_2$ (99.999%) or pure O$_2$ (99.995%). ZnO:Ga exposed to plasma using hydrogen will be referred to as ZnO:Ga-H and oxygen plasma-treated as ZnO:Ga-O.

2.3 AFM-IN-SEM MEASUREMENTS AND CORRELATION OF DATA

Colloidal suspensions of ZnO:Ga, ZnO:Ga-H and ZnO:Ga-O were prepared using HPLC H_2O (p-lab) and sonicated before use (160 W, 37 kHz, Sonorex Digitec, Bandelin). 10 µL of 10 µg/mL of each test sample was dropcast onto a single pre-cleaned silicon substrate (10 x 10 mm^2) for analysis. AFM (LiteScope, NenoVision s.r.o.) fitted with self-sensing probes [12] was fixed directly onto the sample holder of the SEM (Evo 10, Carl Zeiss spol. s.r.o.). The AFM operates inside the SEM chamber under vacuum using the tuning fork method of measurement. An electrical signal is used to oscillate the self-sensing probe [12]. The resonant frequency of oscillations depends on the distance between the probe apex and the surface, and the changes in resonant frequency during probe movement across the surface (x- and y-direction) are compensated by the feedback loop. The feedback loop changes the z-position of the self-sensing probe by trying to keep the resonant frequency constant, thus recording the topographical information. A setpoint frequency of 15 Hz was used because during preliminary measurements the tip lost contact with the surface for setpoint values < 15 Hz. Higher setpoint values (> 15 Hz) only increased tip contamination and did not improve the quality of the topographical information. Variable scan speeds were employed for more efficient data acquisition over the scan area (20 x 20 µm): 1 µm/s scan speed was used to obtain information over the nanorods whereas a faster scan speed (10 µm/s) was used over the remaining area of substrate without the nanorod. It was possible to simultaneously acquire SE and BSE emission signals from the same nanorod using SEM 'spot mode', whereby the electron beam remains in one 'spot' and the sample moves by way of the motorized AFM stage so that both techniques can analyze the same area with a defined offset to ensure that neither technique interferes with the other. SEM parameters were the same for each test sample: accelerating voltage = 10 kV, working distance = 8.0 mm, magnification = 10 kx, current probe = 100 pA, SE brightness = 50 % and contrast = 27 %, BSE brightness = 50 % and contrast = 45 %). The alignment on the topographical and electronic emission information was performed using NenoView software [13] that was necessary because of the defined offset. Minor scan artifacts were removed using Gwyddion software [14] without altering the raw data before 3D CPEM creation that overlaid either SE or BSE emission intensity onto the topographical data, where the electronic emission intensity determined the color scale (color palette: Code-V). The maximum electron emission intensity value was used for setting the same color scale for all 3D CPEM images.

3. RESULTS & DISCUSSION

Navigation of the AFM probe using the high magnification offered by SEM enabled quick targeting of individual nanorods. The topographical information and the electronic emission data were collected from all test samples located on the same substrate and analysed under the same conditions using the same settings. It was particularly important to keep the brightness and contrast settings the same for SE and BSE emission acquisition because the signal intensity governs the color scale used in the 3D CPEM images. Note that varying the brightness or contrast settings does not influence the absolute electronic emission from the sample but does influence the output data used to define the color scale. Therefore, when the brightness and contrast settings are constant for samples that are in focus, any observed differences in SE and BSE emission intensity must be due to differences in material structure [15].
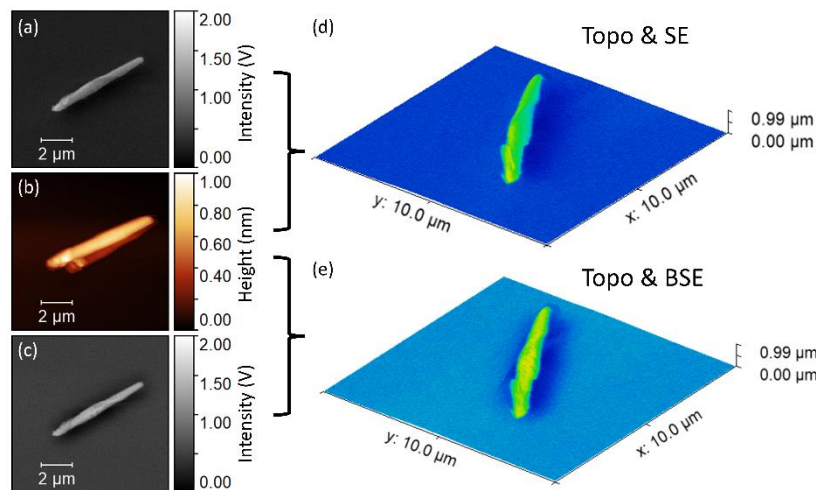
The results from the correlative analyses of ZnO:Ga can be seen in **Figure 2**. The two types of electrons that are typically detected using SEM differ in their origin; SE are generally emitted from the surface whereas BSE originate from deeper within the sample. The SE emission intensity peaked at 1.8 V and BSE emission at 2.0 V, which were the greatest values measured from all test samples (n.b. ZnO:Ga-O also recorded BSE emission intensity of 2.0 V). The lower value of SE intensity relative to BSE intensity is due to the fact that SE originate from inelastic collisions and have less energy compared to BSE that result from elastic collisions. The maximum nanorod height measured from topography was approximately 0.8 µm. It is obvious from both the 3D CPEM images that the electronic emission intensity was greatest from the central region of the nanorod and not the edges. The nanorod width measured using AFM was greater than the nanorod width observed by

SEM because of the finite size of the AFM tip. This also explains the thinner emission intensity from SE and BSE that does not completely cover the entire area of the nanorod in the 3D CPEM images.
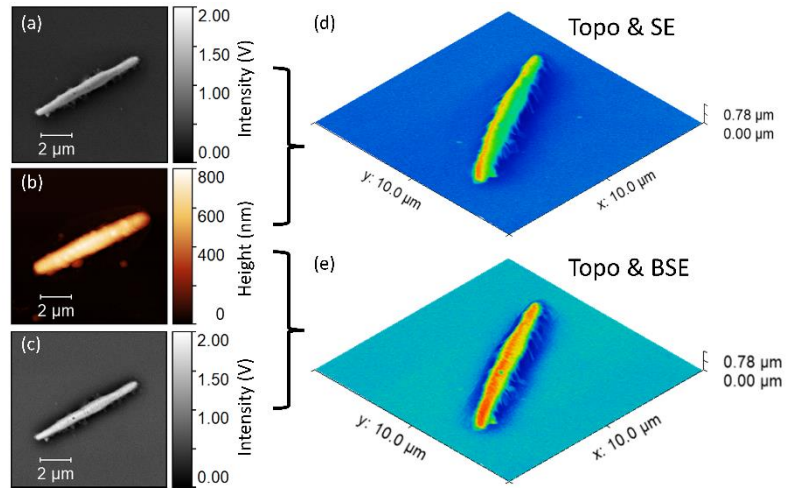
Figure 2 Correlative analysis of ZnO:Ga.(a) SE emission (SEM), (b) topography (AFM), (c) BSE emission (SEM), (d) CPEM image combining (a) & (b) and (e) CPEM image combining (b) & (c).

Interestingly, ZnO synthesized by the hydrothermal growth technique without the addition of a gallium precursor resulted in the creation of small needle-like clusters instead of individual rods [16]. It is clear that the addition of gallium increased the size and altered the form of the hydrothermally-synthesized ZnO, which is in good agreement with other ZnO nanostructures in the presence of a dopant using the same technique [17].
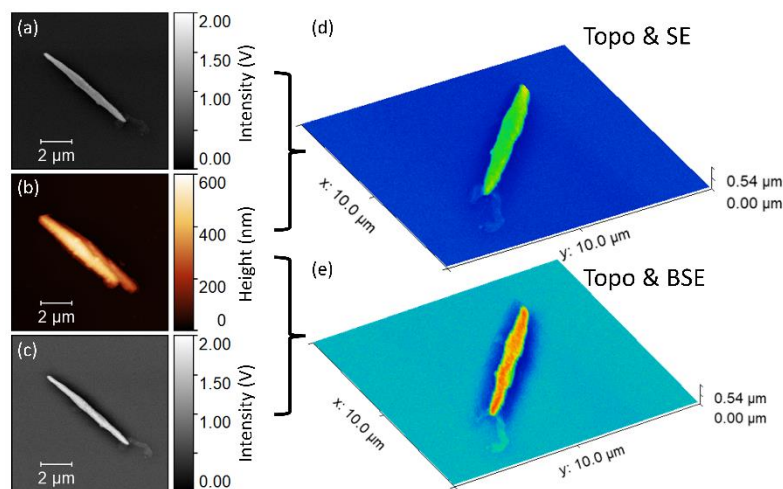

Figure 3 Correlative analysis of ZnO:Ga-H. (a) SE emission (SEM), (b) topography (AFM), (c) BSE emission (SEM), (d) CPEM image combining (a) & (b) and (e) CPEM image combining (b) & (c).

The results from the correlative analysis of ZnO:Ga-H can be seen in **Figure 3**. Plasma treatment by hydrogen did not change the size or shape of the material but it did change the rod surface. Both maximum SE emission and BSE emission intensity (1.5 V) were lower relative to ZnO:Ga. The topography scan shows two nanorods with a maximum nanorod height of approximately 1 µm, however there was only one nanorod detected from the SEM images. This is a result of AFM tip contamination that created a second 'ghost' nanorod. Plasma treatment typically etches material from the surface due to heavy ion bombardment and differences in surface structure can influence the measured absolute electron emission. However, zinc (30) and gallium (31) have

very similar atomic numbers, and hence electron orbital structures, therefore it would be difficult to differentiate between the electronic emission from both these elements using SEM.

Figure 4 shows the results from the correlative analysis of ZnO:Ga-O which displays the same (lowest observed) value of SE emission as ZnO:Ga-H (i.e., 1.5 V), yet the same (greatest observed) value of BSE emission as ZnO:Ga (i.e., 2.0 V). Similar to ZnO:Ga-H, the topography scan shows two nanorods however there was only one nanorod detected from the SEM images. This is again a result of AFM tip contamination that created a second 'ghost' nanorod. Tip contamination is a recuring problem in AFM scans that introduces unwanted artifacts [18]. Attempts have been made to modify the surface of the tip with the aim of reducing the prevalence of such artifacts, for example to reduce the adhesive properties [19] or increase the surface hydrophobicity of the tip [20]. The common objective is to try and minimise tip-surface interaction without jeopardising the image resolution or quality. Similar to ZnO:Ga and ZnO:Ga-H, the colorized 3D CPEM images that combined topography with SE or BSE emission shows the most intense signal was produced along the entire length from the upper central region and not towards the edges.

Since the topography of all analyzed nanorods are of similar size and shape and exhibit similar features, the differences observed in SE and BSE emission contrast must be related to subtle material and chemical modifications as a result of plasma treatments. The main aim of the current research was to correlate the information obtained from the same nanorods by separate techniques, and the effect of plasma treatment on the properties of ZnO:Ga is a matter of ongoing analyses by spectroscopic methods and beyond the scope of this work.

Figure 4 Correlative analysis of ZnO:Ga-O. (a) SE emission (SEM), (b) topography (AFM), (c) BSE emission (SEM), (d) CPEM image combining (a) & (b) and (e) CPEM image combining (b) & (c).

4. CONCLUSION

We presented true *in-situ* correlation between topographical information obtained from AFM with SE and BSE emission data simultaneously acquired from the same nanorods analyzed under the same conditions and brightness/contrast settings to produce 3D CPEM images. This approach provided added information regarding the location of SE and BSE emission relative to surface topography of ZnO:Ga. The maximum SE and BSE emission intensity was measured from ZnO:Ga without plasma treatment and originated from along the central region of the nanorod. Plasma treatment did not change the location of the maximum emission intensity but did influence the absolute values. Hydrogen plasma treatment reduced both SE and BSE emission intensity relative to ZnO:Ga, whereas oxygen plasma treatment only reduced SE emission. This direct

correlation of electronic emission and plasma treatment may help elucidate various optical as well as biological interactions of ZnO:Ga nanorods.

ACKNOWLEDGEMENTS

REFERENCES

[1] CAPLAN, J., NIETHAMMER, M., TAYLOR, R. M. and CZYMMEK, K. J. The power of correlative microscopy: multi-modal, multi-scale, multi-dimensional. *Current Opinion in Structural Biology.* 2011, vol. 21, pp. 686-93.

[2] LOUSSERT FONTA, C. and HUMBEL, B. M. Correlative microscopy. *Archives of Biochemistry and Biophysics*. 2015, vol. 581, pp. 98–110.

[3] NEUMAN, J., NOVACEK, Z., PAVERA, M. and NOVOTNA, V. Correlative Probe and Electron Microscopy CPEM™ - The Novel Technology for 3D Material Surface Analysis. *Microscopy and Microanalysis.* 2019, vol. 25, pp. 430-1.

[4] MICOVA, J., REMES, Z., ARTEMENKO, A., BURYI, M., LEBEDA, M. and CHANG, Y. Y. Plasma Treatment of Ga-Doped ZnO Nanorods. *Physica status solidi (a).* 2022, vol. 219, 2100663.

[5] VANDENABEELE, C. R. and LUCAS, S. Technological challenges and progress in nanomaterials plasma surface modification - A review. *Materials Science and Engineering: R: Reports.* 2020, vol. 139, 100521.

[6] REMES, Z., ARTEMENKO, A., UKRAINTSEV, E., SHARMA, D. K., BURYI, M., KROMKA, A., POTOCKY, S., SZABO, O., KULICEK, J., REZEK, B., PORUBA, A., MICOVA, J. and SHU HSU, H. Changes of Morphological, Optical, and Electrical Properties Induced by Hydrogen Plasma on (0001) ZnO Surface. *physica status solidi (a).* 2022, vol. 219, 2100427.

[7] TOLUBAYEVA, D. B., GRITSENKO, L. V., KEDRUK, Y. Y., AITZHANOV, M. B., NEMKAYEVA, R. R. and ABDULLIN, K. A. Effect of Hydrogen Plasma Treatment on the Sensitivity of ZnO Based Electrochemical Non-Enzymatic Biosensor. *Biosensors.* 2023, vol. 13, 793.

[8] KONDRATOWICZ, I., NADOLSKA, M., ŞAHIN, S., ŁAPIŃSKI, M., PRZEŚNIAK-WELENC, M., SAWCZAK, M., YU, E. H., SADOWSKI, W. and ŻELECHOWSKA, K. Tailoring properties of reduced graphene oxide by oxygen plasma treatment. *Applied Surface Science.* 2018, vol. 440, pp. 651-9.

[9] MA, C., NIKIFOROV, A., HEGEMANN, D., DE GEYTER, N., MORENT, R. and OSTRIKOV, K. (Ken). Plasma-controlled surface wettability: recent advances and future applications. *International Materials Reviews.* 2023, vol. 68, pp. 82-119.

[10] XUE, Y., HE, H., JIN, Y., LU, B., CAO, H., JIANG, J., BAI, S. and YE, Z. Effects of oxygen plasma treatment on the surface properties of Ga-doped ZnO thin films. *Appl. Phys. A* 2014, vol. 114, pp. 509-13.

[11] RUTHERFORD, D., REMEŠ, Z., KOLAROVA, K., MATOLÍNOVÁ, I., ČECH, J., MICOVA, J. and REZEK, B. Enhanced Antimicrobial and Photocatalytic Effects of Plasma-Treated Gallium-Doped Zinc Oxide. *Applied Surface Science.* 2023. (accepted for publication 30/01/24)

[12] AKIYAMA, T., STAUFER, U., DE ROOIJ, N. F., LANGE, D., HAGLEITNER, C., BRAND, O., BALTES, H., TONIN, A. and HIDBER, H. R. Integrated atomic force microscopy array probe with metal-oxide-semiconductor field effect transistor stress sensor, thermal bimorph actuator, and on-chip complementary metal-oxide-semiconductor electronics. *Journal of Vacuum Science & Technology B: Microelectronics and Nanometer Structures Processing, Measurement, and Phenomena.* 2000, vol. 18, pp. 2669-75.

[13] NOVOTNA, V., HORAK, J., KONECNY, M., HEGROVA, V., NOVOTNY, O., NOVACEK, Z. and NEUMAN, J. AFM-in-SEM as a Tool for Comprehensive Sample Surface Analysis. *Microscopy Today.* 2020, vol. 28, pp. 38-46.

[14] NEČAS, D. and KLAPETEK, P. Gwyddion: an open-source software for SPM data analysis. *Open Physics.* 2012, vol. 10, pp. 181-8.

[15]   HASHIMOTO, Y., ITO, H. and SASAJIMA, M. Enhancement of image contrast for carbon nanotube and polymer composite film in scanning electron microscope. *Microscopy.* 2020, vol. 69, pp. 167-72.

[16]   MIČOVÁ, J., BURYI, M., ŠIMEK, D., DRAHOKOUPIL, J., NEYKOVA, N., CHANG, Y.-Y., REMEŠ, Z., POP-GEORGIEVSKI, O., SVOBODA, J. and IM, C. Synthesis of zinc oxide nanostructures and comparison of their crystal quality. *Applied Surface Science.* 2018, vol. 461, pp. 190-5.

[17]   NADEEM, M. S., MUNAWAR, T., MUKHTAR, F., NAVEED UR RAHMAN, M., RIAZ, M., HUSSAIN, A. and IQBAL, F. Hydrothermally derived co, Ni co-doped ZnO nanorods; structural, optical, and morphological study. *Optical Materials.* 2021, vol. 111, 110606.

[18]   GOŁEK, F., MAZUR, P., RYSZKA, Z. and ZUBER, S. AFM image artifacts. *Applied Surface Science.* 2014, vol. 304, pp. 11-9.

[19]   TAO, Z. and BHUSHAN, B. Surface modification of AFM silicon probes for adhesion and wear reduction. *Tribol Lett.* 2006, vol. 21, pp. 1-16.

[20]   HAOCHIH LIU, B. and CHEN, C.-H. Direct deformation study of AFM probe tips modified by hydrophobic alkylsilane self-assembled monolayers. *Ultramicroscopy.* 2011, vol. 111, pp. 1124-30.